The Electronic Structure of Copper in the Polymer Potassium Bis(carbonato)cuprate(II) as determined from Precise *X*-Ray Diffraction Data

By **Brian N. Figgis, Philip A. Reynolds, Allan H. White,** and **Geoffrey A. Williams,**† School of Chemistry, University of Western Australia, Nedlands, Western Australia, Australia 6009

The crystal structure of the polymer potassium bis(carbonato)cuprate(II), $K_2[Cu(CO_3)_2]$, has been investigated in terms of the electronic structure of the copper atom. Single-crystal *X*-ray diffraction data with $(\sin\theta)/\lambda \leqslant 10.8$ nm^{-1}, which were previously used in a $3\sigma(I)$ refinement of the crystal structure, were employed. Crystals are orthorhombic, space group *Fdd*2, $Z = 8$, $a = 1.142\,5(3)$, $b = 1.765\,8(4)$, $c = 0.615\,4(2)$ nm. All 1 693 independent reflections were used in a least-squares refinement on intensity values. Final agreement indices were R 0.029 and χ 2.027. The copper atom is in an essentially square-planar environment of four oxygen atoms from the bridging carbonato-groups [Cu–O 192.9(1) and 193.3(1) pm]. The final difference-Fourier synthesis showed non-centrosymmetric areas of positive and negative deformation charge density on opposite sides of the CuO_4 'plane.' These regions of charge were included in the scattering model as spherical scatterers, and their populations refined to ±0.31(4) electrons at fixed axial positions 55 pm from the copper atom. The dipole moment on the copper atom, parallel to the *c* crystal axis, is of magnitude $0.5(1) \times 10^{-29}$ C m. The symmetry of these deformation density features does not follow the local (bonded) square-planar symmetry of the copper atom environment. Two Cu · · · CO contacts of *ca.* 280 pm, which occur in only one axial direction, seem to be involved in the polarisation of the valence electrons of the copper atom. The non-centrosymmetry of these deformation density features precludes their modelling in terms of 3*d* or 4*s* atomic orbital populations.

THE study of the chemistry of transition-metal complexes is largely concerned with the redistribution of valence electrons accompanying their formation or reaction. The direct observation of the three-dimensional electron distribution in molecules is possible using precise *X*-ray diffraction data. This is distinct from other experimental techniques, such as spectroscopic measurements, which reflect the energy of the systems involved and only indirectly relate to the spatial properties of the electrons.

Charge-density analyses using accurate *X*-ray diffraction data, often coupled with a neutron diffraction definition of thermal motion, have been successfully performed on a number of compounds containing first- and second-row elements.[1] In the case of transition-metal atoms, the core electron density, which is usually approximated as spherically symmetrical, dominates the scattering process. It is then far more difficult to separate the relatively very small spherical and aspherical components of the valence electron scattering from the dominant core scattering. An accurate modelling of core and valence effects, as well as thermal motion, is required. It has only recently been demonstrated that chemically significant information about transition-metal atom valence electrons can be obtained from accurate *X*-ray diffraction data (ref. 2 and refs. therein).

A major concern in all valence charge-density analyses should be the representation of the results in terms of chemically meaningful parameters. Maps of the residual electron density are essentially only a qualitative means of representing deviations of the valence electrons from that assumed in the modelling process. Their use in explaining or predicting chemical properties is limited. Perhaps the best way we have of presenting results in a form that is readily translated into the other areas of chemical interest is *via* the concept of atomic orbital populations. Two recent *X*-ray studies of transition-metal complexes have presented the results for the transition-metal atoms in terms of 3*d* and, in one case, 4*s* atomic orbital populations.[2,3] The unpaired electron density in a number of transition-metal complexes, determined by the polarised neutron diffraction technique, has also been modelled in terms of metal 3*d* and 4*s* and ligand 2*p* orbital populations.[4–8] This method of analysis is reasonably facile only in cases where the atomic orbitals involved in the covalent bonding on each atom are closely represented by a single set of free-ion atomic orbitals. The scattering from hybrid atomic orbitals has been modelled in certain simple cases, but hybridisation involving *d* orbitals is a problem which has not yet been tackled. We should note that a simple multipole analysis of the charge density cannot be directly translated into a description of the orbital wave functions. It is those wave functions which are the starting point for theoretical chemistry.

The present study of the charge density about the copper atom in $K_2[Cu(CO_3)_2]$, using an accurate *X*-ray diffraction data set already at hand,[9] was undertaken to determine whether modelling of the metal valence electrons in terms of centrosymmetric 3*d* and 4*s* orbitals is appropriate for all metal atoms, including those positioned at a non-centrosymmetric site as is the case here. The crystal structure of ferromagnetic $K_2[Cu(CO_3)_2]$ was previously determined[9] using 1 441 'observed' $[I > 3\sigma(I)]$ data with $(\sin\theta)/\lambda \leqslant 10.8$ nm^{-1}. Refinement on F converged with a residual $R(F)$ of 0.027. The structure consists of potassium cations embedded in an infinite three-dimensional polymeric array of approximately square-planar co-ordinated copper atoms with bridging carbonate groups.

† *Present address*: Australian Radiation Laboratory, Lower Plenty Road, Yallambie, Victoria, Australia 3085.

EXPERIMENTAL

Crystal Data.[9]—$C_2CuK_2O_6$, M 261.8, Orthorhombic, space group $Fdd2$, a 1.142 5(3), b 1.765 8(4), c 0.615 4(2) nm, U 1.241 6(5) nm^3, D_m 2.79(1), Z 8, D_c 2.80 Mg m^{-3}, Mo-K_α radiation (graphite crystal monochromator), λ 71.069 pm, μ 4.70 mm^{-1}, crystal size 0.26 × 0.13 × 0.45 mm, T 295(1) K.

Structure Refinement.—The unique data set with $(\sin\theta)/\lambda \leqslant 10.78$ nm^{-1}, which was used in the previous structure analysis,[9] formed the basis for the refinements. The present refinement differed from the previous one in that all 1 693 independent reflections were used in the analysis. One systematically absent reflection, included in the previous analysis as a ' less-than ', was discarded. Least-squares refinement of atomic co-ordinates and anisotropic thermal parameters was performed by use of the program CRYLSQ [10] in the full-matrix mode. The refinement was based on I_o values so that all measured data, including those observations with intensities experimentally determined as negative, could be included in the least-squares process. This is to be preferred to refinement on F values as it eliminates the bias introduced into data by using a $\sigma(I)$ rejection criterion or by setting all negative intensities to zero.[11] The function minimised was $\Sigma w(\Delta I)^2$ where $\Delta I = I_o - I_c$ and $w = 1/\sigma^2(I_o)$ is the weight assigned to the I_o values. Geometrical and analytical absorption corrections were applied to the I_c values, the latter by use of the program ABSCOR.[10]

Starting atomic parameters were obtained from the previous refinement.[9] Scattering-factor curves for the neutral atoms C, O, and Cu, and for the K^+ ion, were from ref. 12. All scattering factors were modified for the real and imaginary anomalous dispersion corrections.[13] Anisotropic thermal parameters were assigned to all atoms, and in the case of Cu a population parameter was varied. An examination of the I_o and I_c values indicated the total absence of extinction effects, and in a trial refinement the isotropic extinction parameter [10] did not vary significantly from zero.

Refinement (51 variables) converged with R ($= \Sigma|\Delta I|/\Sigma|I_o|$) 0.029 and χ $\{ = [\Sigma w(\Delta I)^2/(n - v)]^{\frac{1}{2}}\}$ 2.027,

TABLE 1

Final atomic position co-ordinates for $K_2[Cu(CO_3)_2]$ at 295 K

Atom	x/a	y/b	z/c
Cu	0	0	0
K	0.578 05(3)	0.200 06(2)	0.196 12(9)
C	0.081 74(13)	0.126 70(8)	0.204 97(36)
O(1)	0.082 68(11)	0.095 40(7)	0.012 86(26)
O(2)	0.101 33(11)	0.199 83(7)	0.213 06(32)
O(3)	0.059 64(12)	0.088 78(8)	0.372 06(28)

where n and v are the numbers of observations and variables respectively. The maximum shift-to-error ratio was 0.006 : 1. Final atomic positional co-ordinates, with estimated standard deviations in parentheses, are listed in Table 1. Anisotropic thermal parameters are listed for Cu in Table 2(*a*), and for all other atoms in Table 2(*b*). The population parameter for Cu refined to 0.981(2). Observed and calculated structure factors are given in Supplementary Publication No. SUP 22920 (10 pp.).*

* For details see Notices to Authors No. 7, *J.C.S. Dalton*, 1979, Index issue.

The absolute configuration of the $K_2[Cu(CO_3)_2]$ structure could not be determined in the previous refinement.[9] We performed a refinement, analogous to that above, using the alternative configuration. At convergence, the values for R and χ were 0.030 and 2.083 respectively. The maximum shift-to-error ratio was 0.006 : 1. This result indicates that the configuration originally reported,[9] and refined above (Table 1 values), is the correct one.

A difference synthesis performed after the above refinement (χ 2.027) showed significant peaks, to a maximum of

TABLE 2

Final thermal parameters (pm^2) for $K_2[Cu(CO_3)_2]$ at 295 K

(*a*) Cu atom anisotropic thermal parameters defined by $T = \exp[-2\pi^2(h^2a^{*2}U_{11} + k^2b^{*2}U_{22} + l^2c^{*2}U_{33} + 2hka^*b^*U_{12} + 2hla^*c^*U_{13} + 2klb^*c^*U_{23})]$

	1 693 Data, conventional refinement	481 Data, $0 < (\sin\theta)/\lambda \leqslant 7.0$ nm^{-1}	972 Data, $8.0 < (\sin\theta)/\lambda < 10.8$ nm^{-1}	1 693 Data, valence refinement *
U_{11}	128.0(9)	133.8(20)	122.5(15)	127.8(8)
U_{22}	85.1(7)	88.7(19)	80.0(14)	85.0(7)
U_{33}	166.2(10)	170.1(23)	159.6(17)	166.9(12)
U_{12}	12.3(10)	12.0(20)	12.5(11)	12.5(9)
U_{13}	0	0	0	0
U_{23}	0	0	0	0

(*b*) Other atomic thermal parameters [defined as in (*a*)]

Atom	U_{11}	U_{22}	U_{33}	U_{12}	U_{13}	U_{23}
K	208(2)	193(1)	249(2)	28(1)	39(1)	29(1)
C	103(4)	123(5)	274(8)	11(4)	−14(5)	−20(6)
O(1)	208(5)	135(4)	252(6)	−18(4)	2(5)	−17(5)
O(2)	168(5)	105(4)	446(9)	−19(3)	−45(6)	−45(5)
O(3)	260(6)	236(6)	258(7)	4(5)	21(6)	37(6)

* This refinement, described in the text, employs spherical regions of positive and negative populations close to the Cu atom, at positions (0, 0, −0.09) and (0, 0, 0.09) respectively.

|0.96| × 10^{-6} e pm^{-3}, close to the Cu atom. Sections of this difference synthesis are shown in Figure 1 (view down the c axis, essentially containing the almost square-planar CuO_4 atomic array), and in Figure 2 (view down the a axis, showing charge density perpendicular to the CuO_4 ' plane '). It is important, when viewing these maps, to remember that they represent departures of the observed electron density from that assumed in the model. Our model assumes spherically symmetric electron densities about stationary atoms, which are smeared by anisotropic thermal motion. Areas of negative charge density therefore represent regions where the average ' spherical atom ' model places too much charge, and *vice versa*. It must also be remembered that part of the asphericity in the valence electron distribution may have been incorporated in the thermal parameters which, ideally, model the asphericity due to thermal motion.

Some qualitative observations can be made from these maps. There are significant areas of charge density more than 100 pm from the Cu nucleus, whereas charge density in a 3d orbital is at a maximum *ca.* 30 pm from the nucleus.[14] Also the expected ' hole ' in the $3d_{x^2-y^2}$ orbital of the d^9 Cu^{II} atom is not well defined (Figure 1). Finally, the charge density perpendicular to the CuO_4 ' plane ' (Figure 2) is non-centrosymmetric and of significant size (|0.9| × 10^{-6} e pm^{-3}). This last feature is intriguing. Although non-centrosymmetric deformation density features have previously been observed, for instance in the tetrahedral CrO_4^{2-} ion,[15] this is the first instance where the symmetry of the deformation density does not follow the local (bonded)

symmetry of the metal-atom environment. Furthermore, the non-centrosymmetry of this feature precludes its modelling in terms of centrosymmetric 3*d* or 4*s* orbitals.

To check that the effect on the thermal parameters of the asphericity in the charge density due to the valence electrons is negligible, separate refinements were performed employing only the high- or low-angle portions of the data. In these refinements (50 variables), the population parameter of Cu was constrained at 0.981. For the 481 data with $0 < (\sin\theta)/\lambda \leqslant 7.0$ nm^{-1}, refinement converged with R 0.028 and χ 3.009. For the 972 data with $8.0 < (\sin\theta)/\lambda < 10.8$ nm^{-1}, refinement converged with R 0.072 and χ 1.192. For all atoms there were only small apparently random differences between the thermal parameters from the two refinements. The values for the Cu atom are presented in Table 2(*a*). Difference syntheses on all the data performed after these refinements showed similar features to those of Figures 1 and 2. We infer that the values of thermal parameters for the Cu atom determined from the refinements are derived only from thermal vibration together with some small thermal diffuse scattering effect. Possible reasons for this are the dominance in the X-ray scattering of the transition-metal core electrons, which are assumed to be spherically symmetric in the absence of thermal effects; and also the fact that most of the valence charge density about the Cu atom is *non-centrosymmetric*, and hence it cannot be modelled at all well by the *centrosymmetric* anisotropic thermal parameters.

The features present in the deformation density maps (Figures 1 and 2) were obviously not amenable to modelling in terms of centrosymmetric 3*d* or 4*s* orbital functions. The method of analysis previously successfully applied [2,4-8] to metal atoms in centrosymmetric sites therefore could not be used here. To obtain valence orbital electronic populations for the Cu atom seems difficult as hybrid orbitals of some type must be involved. However, in order to quantify the features in the maps somewhat, an attempt was made to include in the scattering model the areas of positive and negative charge perpendicular to the CuO_4 ' plane ' (Figure 2). This was done by including two spherically symmetrical regions, one of positive and one of negative population, on either side of the CuO_4 ' plane ', at fixed positions (0, 0, −0.09) and (0, 0, 0.09) respectively. Such positions were indicated by the difference–Fourier synthesis. A number of trial refinements determined that the features were rather sharp and the K^+ scattering curve (with an appropriate scale) was chosen to represent the scattering-factor curve. This scattering curve was modified by a refineable isotropic Gaussian function of the form $\exp[-8\pi^2U(\sin^2\theta)/\lambda^2]$. These regions of charge were constrained to have identical U values, and the populations were constrained to be equal in magnitude but of opposite sign.

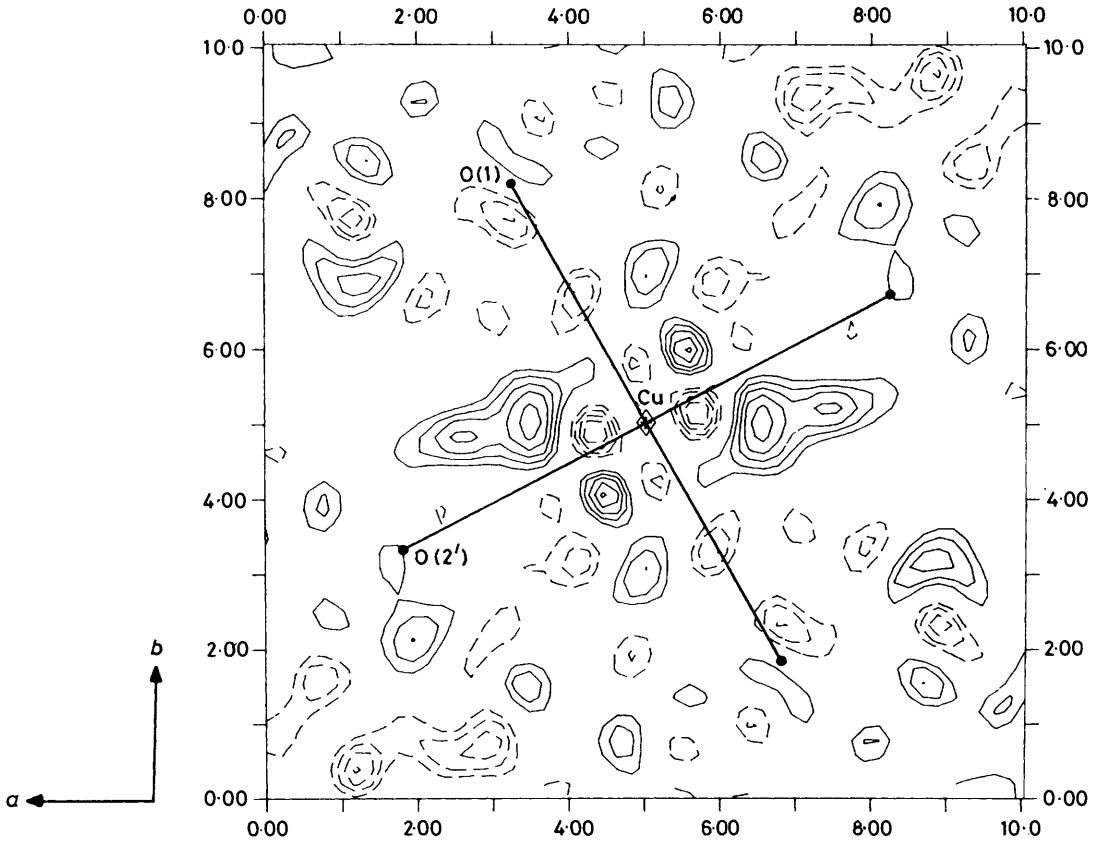

FIGURE 1 Deformation charge-density section in the *ab* crystal plane for $K_2[Cu(CO_3)_2]$. The copper atom and four co-ordinated oxygen atoms are shown as projections onto this plane. Atoms O(1) and O(2') are 7.9(2) and −22.7(2) pm respectively from the plane. The contour interval is 0.1×10^{-6} e pm^{-3}. Negative contours are dashed. The zero and $\pm 0.1 \times 10^{-6}$ e pm^{-3} contours have been omitted for clarity. The scales along the edges are in atomic units (1 atomic unit = 52.918 pm)

This refinement (53 variables) converged with R 0.029, χ 1.952, and a maximum shift-to-error ratio of 0.3 : 1. At convergence, the populations of the regions were 0.31(4) and −0.31(4) electrons. The U value, −41(28) pm², merely provides a representation of the scattering factor for the regions by that of K^+, and has no other physical meaning. The population parameter of the Cu atom refined to 0.982(2) and anisotropic thermal parameters for Cu from this refinement are presented in Table 2(*a*). Each region was positioned 55 pm from the nucleus of the Cu atom. The fact that the χ value for this refinement is lower than that for the conventional refinement indicates that this ' valence electron ' model provides a better fit to the observed intensity data.

We also attempted to refine the positions (z co-ordinates) of the regions of charge together with the populations and U value. This refinement converged with the regions centred 46(4) pm from the Cu atom and with populations of ±0.56(10) electrons and a U value of 217(48) pm². However, the agreement factors were higher (R 0.030, χ 1.989) than for the refinement presented above.

DISCUSSION

The structure of $K_2[Cu(CO_3)_2]$ consists of potassium cations embedded in an infinite three-dimensional polymeric array of almost square-planar co-ordinated copper atoms with bridging carbonato-ligands.[9] The immediate copper environment is shown in Figures 3 and 4, and the atom-numbering scheme is indicated. Interatomic distances and angles are given in Tables 3 and 4. Except for an increase in precision, due to the inclusion of all measured data in the present refinement, the compound geometry is essentially unchanged from that previously reported.[9]

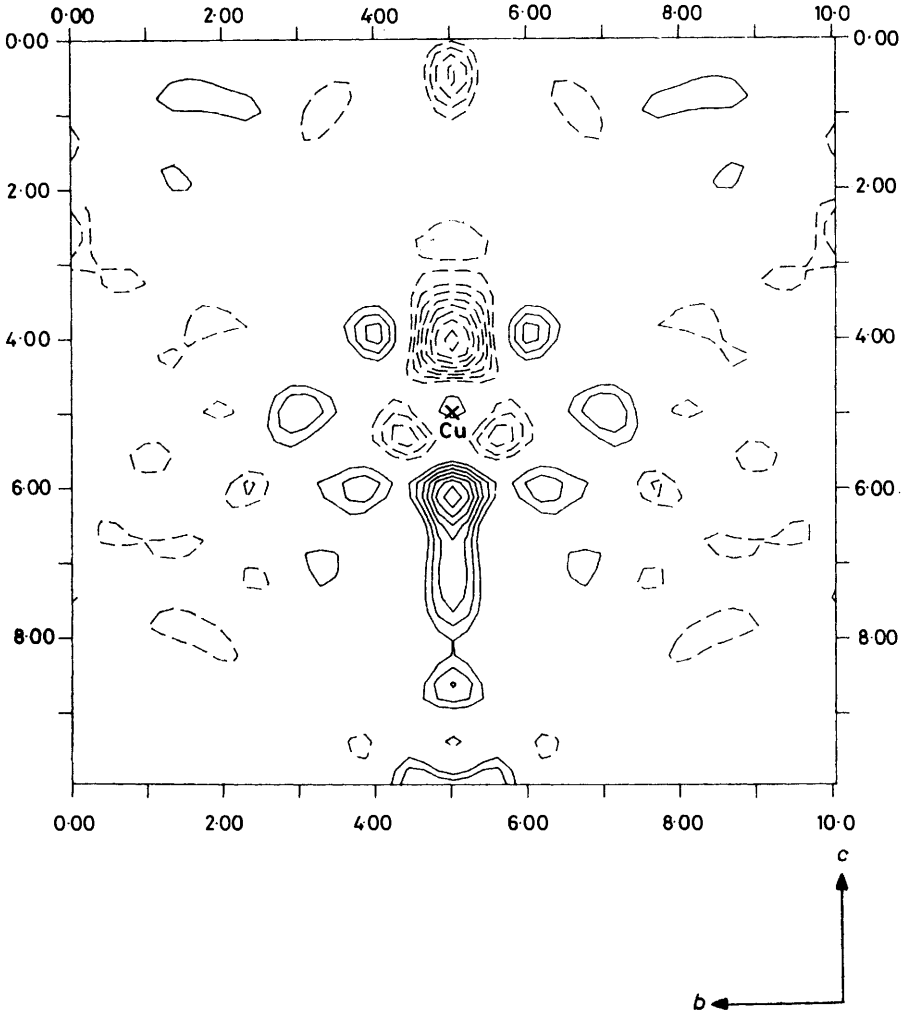

FIGURE 2 Deformation charge-density section in the *bc* crystal plane for $K_2[Cu(CO_3)_2]$. The position of the copper atom is shown. Contours and scales are as described in Figure 1

The interesting feature in this compound is the non-centrosymmetric arrangement of significantly sized areas of charge density perpendicular to the CuO_4 ' plane ' (Figure 2). The symmetry of this deformation density does not follow the approximate locally bonded symmetry (C_{2h}) of the copper-atom environment. An analysis of the copper environment (Figure 4) indicates

that there is indeed a departure from centrosymmetry in the CO_3 groups surrounding the copper atom. On one side of the CuO_4 ' plane ' there are two C–O(3) bonds bent *towards* the axial position about copper, whereas

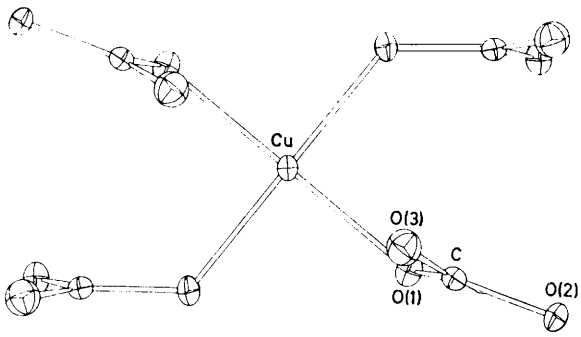

FIGURE 3 An ORTEP drawing, viewed along the *c* crystal axis, showing the copper-atom environment in $K_2[Cu(CO_3)_2]$ and atom numbering. Thermal ellipsoids are drawn at the 40% probability level. A more complete representation of the unit-cell contents is given in ref. 9

on the other side of the plane the C–O(3) bonds are bent *away* from the axial position. However, these C–O(3) contacts with copper on the one side of the CuO_4 ' plane ' are at *ca.* 280 pm, which is considerably longer than the usual distance of *ca.* 190 to 210 pm for conventional bonding between these atoms.

If it is assumed that electrostatic interactions, however, are still very significant at distances such as 280 pm, then it is possible that the electronegative C–O(3) bonds on the one side of the CuO_4 ' plane ' are responsible for a polarisation of the valence electrons of the copper atom. We would then expect a net transfer of negative charge onto the side of the CuO_4 ' plane ' away from the C–O(3) contacts. This is found. The negative region of deformation density in Figure 2, which corresponds to an *excess* amount of charge placed there by the spherical thermally smeared atom model, lies on the same side of the CuO_4 ' plane ' as the two C–O(3) close contacts with copper. Such a classical, electrostatic model neglects all quantum effects and should not be taken as more than a convenient hypothesis. Other close contacts (Table 3) which the copper atom has are with two potassium cations on the same side of the CuO_4 ' plane ' as the C–O(3) close contacts [Cu · · · K 348.9(1) pm], and with two potassium cations on the opposite side of the ' plane ' [Cu · · · K 386.5(1) pm]. The net dipolar field at the copper atom due to these four surrounding potassium cations is presumably small.

TABLE 3

Interatomic distances (pm) in $K_2[Cu(CO_3)_2]$ at 295 K *

	All 1 693 data, conventional refinement	Previous $3\sigma(I)$ refinement
Cu–O(1)	193.3(1)	193.4(2)
Cu–O(2′)	192.9(1)	193.6(2)
C–O(1)	130.5(3)	130.3(3)
C–O(2)	131.1(2)	130.7(2)
C–O(3)	125.3(3)	125.9(3)
Cu · · · C	273.3(2)	
Cu · · · O(3)	285.7(2)	
Cu · · · O(2)	393.8(1)	
Cu · · · C′	291.8(1)	
Cu · · · O(1′)	363.8(1)	
Cu · · · O(3′)	366.1(2)	
Cu · · · K′	386.5(1)	
Cu · · · K″	348.9(1)	

* All Cu contacts within 400 pm are given. Primed and double-primed atoms are related by the co-ordinate transformations $(\frac{1}{4} - x, -\frac{1}{4} + y, -\frac{1}{4} + z)$ and $(\frac{3}{4} - x, -\frac{1}{4} + y, \frac{1}{4} + z)$ respectively.

TABLE 4

Angles (°) in $K_2[Cu(CO_3)_2]$ at 295 K *

O(1)–Cu–O(2′)	88.55(5)	O(1″)–Cu · · · C	149.49(6)
O(1)–Cu–O(1″)	175.31(7)	O(1″)–Cu · · · O(3)	124.18(6)
O(1)–Cu–O(2‴)	92.00(5)	O(2‴)–Cu · · · C	88.82(5)
O(2′)–Cu–O(2‴)	166.46(8)	O(2‴)–Cu · · · O(3)	93.01(6)
O(1)–Cu · · · C	25.93(6)	O(1)–C–O(2)	116.7(2)
O(1)–Cu · · · O(3)	51.14(6)	O(1)–C–O(3)	121.3(2)
O(2′)–Cu · · · C	97.44(5)	O(2)–C–O(3)	122.0(2)
O(2′)–Cu · · · O(3)	97.84(6)		

* Primed, double-primed, and triple-primed atoms are related to the unprimed atom by the operations $(\frac{1}{4} - x, -\frac{1}{4} + y, -\frac{1}{4} + z)$, $(-x, -y, z)$, and $(-\frac{1}{4} + x, \frac{1}{4} - y, -\frac{1}{4} + z)$ respectively.

From the refinement including the regions of charge perpendicular to the CuO_4 ' plane ' in the scattering model, we can estimate the dipole moment on the copper atom. It is almost parallel to the *c* crystal axis, and of magnitude $0.5(1) \times 10^{-29}$ C m [34(4) electron pm] with the charge centroids separated by 110 pm.

As already mentioned, the deformation charge-density features perpendicular to the CuO_4 ' plane ' have incorrect symmetry for occupancy of 3*d* or 4*s* orbitals, and it is necessary to invoke hybridisation such as *sp* or *pd* type to explain the observed non-centrosymmetry. The deformation charge density in the crystal

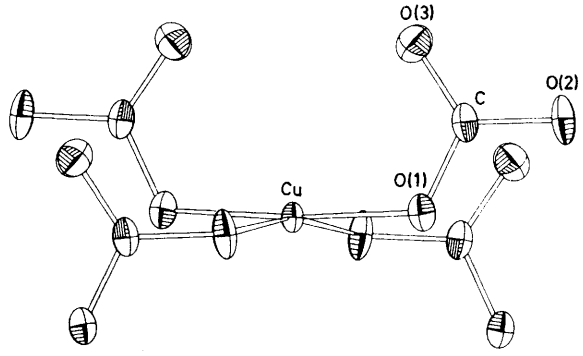

FIGURE 4 An ORTEP drawing, viewed along the *a* crystal axis, showing the copper-atom environment in $K_2[Cu(CO_3)_2]$ and atom numbering. Thermal ellipsoids are drawn at the 30% probability level

ab plane (essentially the CuO_4 ' plane '), shown in Figure 1, also cannot be readily interpreted in terms of pure 3*d* and 4*s* orbital populations. In this plane, there is a general expansion of the electron density from the model of a thermally smeared Cu^0 atom with a population parameter of 0.981 (which indicates an approximate charge of +0.6 e on the copper atom). The areas of negative deformation density (electron deficiencies) close to the copper nucleus do not closely resemble the

expected pattern for a ' hole ' in the $3d_{x^2-y^2}$ orbital of the formally $3d^9$ copper(II) centre. These features are less significant than the non-centrosymmetric regions along the *c* axial direction, and could be artefacts.

We acknowledge support from the Australian Research Grants Committee. G. A. W. thanks the Australian Institute of Nuclear Science and Engineering for a Research Fellowship. We thank Dr. E. N. Maslen for stimulating discussions.

[0/1053 *Received*, 7th *July*, 1980]

REFERENCES

[1] See for example, the review papers in *Israel J. Chem.*, 1977, **16**, 87—229.
[2] B. N. Figgis, E. S. Kucharski, and G. A. Williams, *J.C.S. Dalton*, 1980, 1515.
[3] E. D. Stevens and P. Coppens, *Acta Cryst.*, 1979, **A35**, 536.
[4] B. N. Figgis, R. Mason, A. R. P. Smith, and G. A. Williams, *J. Amer. Chem. Soc.*, 1979, **101**, 3673.
[5] B. N. Figgis, P. A. Reynolds, and G. A. Williams, *J.C.S. Dalton*, 1980, 2348.
[6] B. N. Figgis, P. A. Reynolds, and G. A. Williams, *J.C.S. Dalton*, 1980, 2339.
[7] G. A. Williams, B. N. Figgis, and R. Mason, *J.C.S. Dalton*, in the press.
[8] B. N. Figgis, J. B. Forsyth, R. Mason, and G. A. Williams, in preparation.
[9] A. Farrand, A. K. Gregson, B. W. Skelton, and A. H. White, *Austral. J. Chem.*, 1980, **33**, 431.
[10] J. M. Stewart, 'The *X*-Ray System,' Version of March 1976, Technical Report TR-446, Computer Science Centre, University of Maryland.
[11] F. L. Hirshfeld and D. Rabinovich, *Acta Cryst.*, 1973, **A29**, 510.
[12] D. T. Cromer and J. B. Mann, *Acta Cryst.*, 1968, **A24**, 321.
[13] D. T. Cromer and D. Liberman, *J. Chem. Phys.*, 1970, **53**, 1891.
[14] E. Clementi and C. Roetti, *At. Data Nucl. Data Tables*, 1974, **14**, 177.
[15] K. Toriumi and Y. Saito, *Acta Cryst.*, 1978, **B34**, 3149.